High Temp. Mater. Proc., Vol. **30** (2011), pp. 473–483 DOI 10.1515/HTMP.2011.070

Crystallization of the Amorphous Ferric Arsenate in the Saturated Steam Atmosphere

Hideyuki Itou,[1] **Tomio Takasu**[1,*] **and Yasunori Ueno**[1]

[1] Department of Materials Science and Engineering, Kyushu Institute of Technology, Kitakyushu, Japan

Abstract. Scorodite is an appropriate compound for the immobilization of arsenic generated in the nonferrous smelting and refining industry. To develop processes to produce scorodite, the mechanism of scorodite formation is important. As a part of the mechanism elucidation of the scorodite formation, crystallization of the amorphous ferric arsenate into scorodite was investigated in the gas atmospheres. The amorphous sample was prepared by the precipitation from the solution of Fe(III) and As(V) at 35°C. The sample was composed of the weak agglomerates around 10 μm which consisted of particles of about 1 μm in diameter. In the dry atmosphere, the crystallization did not occur. However, in the saturated steam atmosphere, the crystallization of the amorphous into the scorodite occurred at 95°C. The higher temperature accelerated the crystallization in terms of the incubation period and crystallinity. The crystallinity of the sample formed at 160°C for 3 h was the same as that of the hydrothermally synthesized scorodite. The start of the crystallization was always coincident with the start of the increase in particle size. It suggested that the increase in particle size contributed to the crystallization.

Keywords. Scorodite, crystallization, solid state transformation, steam, amorphous, mechanism.

PACS®(2010). 64.70.dg, 81.20.Ka, 81.30.Mh, 81.20.Ev.

1 Introduction

Arsenic reports in the fly ashes and liquid wastes in the nonferrous smelting and refining industry. The generation of arsenic is increasing because the arsenic concentration in the ores is increasing and the concentrations of the target metals are decreasing. It is necessary to immobilize arsenic in the stable form against the elution.

Scorodite ($FeAsO_4 \cdot 2H_2O$), which is the crystalline hydrated ferric arsenate, has the following characteristics: low solubility, high density and superior filtration property. Therefore, it is an appropriate compound for the arsenic immobilization. On the other hand, the amorphous ferric arsenate is not suitable for the arsenic immobilization due to the high solubility. To produce scorodite, hydrothermal processes using autoclaves [1] are popular but are high-cost.

It is known that scorodite can be produced even less than 100°C (= 373 K) under the atmospheric pressure [2]. To achieve the scorodite production, it is required to prevent the amorphous formation by keeping super-saturation low and to use seed crystals.

Moreover, a novel process to precipitate scorodite was proposed using the injection of an oxidizing gas into aqueous Fe(II) and As(V) solution. It is known that high-quality scorodite is obtained [3,4]. Effects of various factors on the novel process and the product were studied [5–8].

On the other hand when a concentrated solution of Fe(III) and As(V) is retained at 95°C, amorphous ferric arsenate is generated in the early stage but changed to scorodite as time passed [9]. In all the above-mentioned processes, it may be said that the formation of amorphous influences the formation of the scorodite directly or indirectly.

For the crystallization of the amorphous ferric arsenate in the solution, two routes can be considered; (1) dissolution-preciptation and (2) the solid state transformation. On the route (1), the amorphous dissolves into the solution owing to its high solubility, which is followed by the scorodite precipitation from the solution owing to its low solubility. On the route (2), the amorphous changes to crystals in the solid state.

As an easy method to separate these two routes, a preliminary experiment was carried out to hold an amorphous ferric arsenate in a gas atmosphere at 95°C. It was found that the crystallization does occur.

Therefore the effects of retention conditions such as atmosphere and the temperature on the crystallinity and particle size were investigated to acquire the basic knowledge of the crystallization of the amorphous ferric arsenate in the gas atmosphere.

2 Experimental

2.1 Preparation of the Initial Samples

Three types of samples were prepared as the initial samples of the crystallization experiments. The preparation procedure of each initial sample is shown below.

Corresponding author: Tomio Takasu, Department of Materials Science and Engineering, Kyushu Institute of Technology, Sensui 1-1, Tobata, Kitakyushu, 804-8550, Japan;
E-mail: takasu@copper.matsc.kyutech.ac.jp.

Received: March 6, 2011. Accepted: April 15, 2011.

2.1.1 Powder of the Amorphous Hydrated Ferric Arsenate (A)

The ferric sulfate hydrate was used as an iron source and arsenic acid disodium heptahydrate as an arsenic source. These were dissolved in distilled water individually and pH of each solution was adjusted at 1.5 with NaOH and H_2SO_4. Two solutions were mixed at the volume ratio of 1.0. The concentration of each solution was decided so that the concentrations after the mixing became 0.3 mol/L (0.3×10^3 mol/m^3) for both Fe and As. The pH of the solution just after the mixing was 1.0. A 300 mL mixture in a beaker was kept at 35°C in a thermostatic water bath and was retained under agitation in 300 rpm for 24 h. After the retention, the precipitate was separated from the solution using a suction filter with the membrane filter of 1 μm aperture. The precipitate was washed three times by repulp washing with distilled water of 40 mL, and was dried at 35°C at least for two days before using it as an initial sample for the crystallization experiment. This is called the sample A.

2.1.2 Powder Compact of the Amorphous Hydrated Ferric Arsenate (B)

To obtain a better contact between the particles, the powder sample A was pressed to form a compact. A 0.2 g of the sample A was placed in an aluminum ring and pressed by force of 9.8 kN to form a disc with diameter of 14 mm and height of 1mm. The voidage was estimated to be 60% when the density of 3.2313 Mg/m^3 for scorodite was used. This compact is called the sample B. The voidage of the sample A (without the pressure forming) was 67%.

2.1.3 Powder of the Amorphous Dehydrated Ferric Arsenate (C)

The amorphous dehydrated ferric arsenate was prepared by retaining the sample A in a dryer at 120°C for 24 h. The temperature for the dehydration was decided by a TG (thermo-gravimetry) result of the sample A as explained in Section 3.1.1. This is called the sample C.

2.2 Crystallization Experiments

The schematic view of the experimental device for crystallization is shown in Figure 1. The initial samples prepared by the procedure explained in Section 2.1 were used for the crystallization experiments. A 0.2 g of the initial sample was placed in a test tube made of glass. The tube was set in a container with water. The container was heated in an electric furnace. When the temperature reached 95°C, the container was closed with the cap, and retained at the scheduled temperature and time. After the retention, it was confirmed that there was no liquid water in the test tube. The sample taken out from the test tube was kept in a dryer at 35°C for two days.

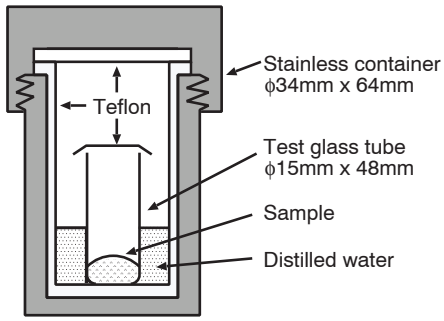

Figure 1. A schematic view of the device for the crystallization experiment.

Experiment	I	II	III	IV	V	VI
Atmosphere	Dry	Humid				
Temperature	95°C			160°C	95°C	160°C
Holding time	1, 3, 6, 9, 12, 24 h				24 h	168 h
Initial sample	A		B	A	C	B
Pressure shaping	×		◯	×		◯
Dehydration	×				◯	×

Table 1. Conditions of the crystallization experiments with the amorphous ferric arsenate. Experiment II was the basic condition of this study. The different conditions from the experiment II were underlined.

Conditions of the crystallization experiments are shown in Table 1. Saturated steam atmosphere was used except in experiment I where a dry air atmosphere was used. In the experiments with the dry atmosphere, water was not placed in the container which was open for the surrounding air atmosphere. Experiment II was the basic condition of this study, with the initial sample A (amorphous hydrated ferric arsenate) and the retention temperature of 95°C. In experiment III, the initial sample B (powder compact) was used. In experiment IV, retention temperature was raised to 160°C. In these experiments, six retention times were examined from 1 h to 24 h.

In experiment V, initial sample C (dehydration) was retained at 95°C for 24 h. In the experiment VI, sample B (powder compact) was retained at 160°C for 168 h.

2.3 Analyses of the Samples

The powder samples were analyzed with XRD and SEM. For samples of the power compacts in the experiments III and VI, both of the surface and the cross section were analyzed with SEM. The compacts were broken into particles with a pestle in a mortar and analyzed with XRD. In the

XRD analyses, the Cu $K\alpha$ line was used and the scanning step angle of 2θ was set to 0.05°. For the XRD analyses, the sample powder was filled in the space with 0.2 mm in depth and 20 mm × 20 mm in area on a glass plate.

TG (thermo-gravimetry) analyses of the samples were conducted in the following conditions: the temperature scanning speed of 10°C/min from a room temperature to 400°C, the N_2-21%O_2 gas flow rate of 100 mL/min, the sample mass around 10 mg.

TEM observation and the electron beam diffraction analyses were carried out on some samples. Concentrations of Fe and As in the sample A were determined by ICP-AES.

3 Results and Discussion

Figure 2 shows XRD patterns obtained in all the experimental conditions and the retention time. Figure 3 shows the corresponding SEM images to Figure 2. In the following section, these results are explained sequentially.

3.1 Analyses of the Prepared Initial Samples

3.1.1 Sample A

The XRD pattern of the initial sample A prepared in Section 2.1.1 is shown in Figure 2 of experimental conditions I, II, IV. The intensity was high around 30° but the peaks were not detected, showing that the prepared sample A is amorphous or very low in crystallinity.

A SEM image of the initial sample A is shown in Figure 3. Weak agglomerates around 10 μm were detected, but it was revealed that the agglomerates consisted of particles of about 1 μm in diameter.

TEM observation results are shown in Figure 4. Any clear spots and rings were not observed in the electron beam diffraction, showing that the sample A was amorphous.

Concentrations measured by ICP-AES are shown in Table 2. The concentrations of Fe and As of the sample were lower than the theoretical concentrations of the scorodite, but the Fe/As mole ratio was found to be equal with that of the scorodite. The water concentration of the sample was estimated at 21.5% from the measured As concentration assuming the chemical formula of $FeAsO_4 \cdot xH_2O$. The concentration was higher than 15.6% of the scorodite.

	Fe (mass%)	As (mass%)	Fe/As (mol ratio)	H_2O (mass%)
Initial sample	23.88	30.20	1.06	21.5*
Scorodite	24.20	32.46	1.00	15.6

* Water content was calculated from the measured As concentration assuming the chemical formula of $FeAsO_4 \cdot xH_2O$.

Table 2. Measured concentrations of the initial sample A.

Results of the TG analyses are shown in Figure 5. The TG result of a scorodite synthesized hydrothermally at 160°C [9] is also shown in Figure 5 for the comparison. The hydrothermally synthesized scorodite showed a remarkable mass reduction above 160°C, and it was 16% at 220°C. This agrees to the mass reduction of 15.6% for the dehydration of the scorodite as expressed in formula (1).

$$FeAsO_4 \cdot 2H_2O \rightarrow FeAsO_4 + 2H_2O. \quad (1)$$

The sample A showed the mass reduction below 100°C, and it was 6% at 95°C and 17% at 220°C. This reduction of 17% was lower than the water concentration of 21.5% as determined by the chemical analysis. It is probably due to shorter drying time for the concentration assay sample (3 days) to achieve the stable water concentration.

Anyway it is clear that the sample A is easy to be dehydrated at the lower temperature in air atmosphere in comparison with scorodite. It could be said that the amorphous hydrated ferric arsenate is easier to be dehydrated because it is a metastable phase [10] with higher free energy than the scorodite. In addition, the dehydration of the amorphous hydrated ferric arsenate was found to be easier than the transformation to the scorodite in the dry atmosphere.

3.1.2 Sample B

The sample B was the pressed compact of the sample A. The SEM images of the surface and inside the disk are shown in Figure 3 of experiment III. It is seen that particles stayed closer than the sample A. It consisted of particles of around 1 μm in diameter, confirming that the particles did not change with the pressure forming.

3.1.3 Sample C

The sample C was prepared by the dehydration of the sample A at 120°C. The TG result is shown in Figure 5. The mass reduction was small below 160°C, but gradually increases above 160°C. This reduction above 160°C was also seen in the sample A. It might be attributed to the impurities which were not able to be washed off, but the cause was not specified because the reduction occurred in the wide temperature range. Nevertheless, the negligible mass reduction below 160°C in the sample A meant that the dehydration was achieved by retention at 120°C for 24 h in air atmosphere.

The XRD pattern of the sample C is shown in Figure 2 of experimental conditions V. The intensity from 20° to 30° became higher than that of the sample A, but any clear peaks were not confirmed, indicating that the sample C was also amorphous.

The SEM image is shown in Figure 3 of condition V. It was the same as the sample A, revealing that the particle appearance did not change with the dehydration.

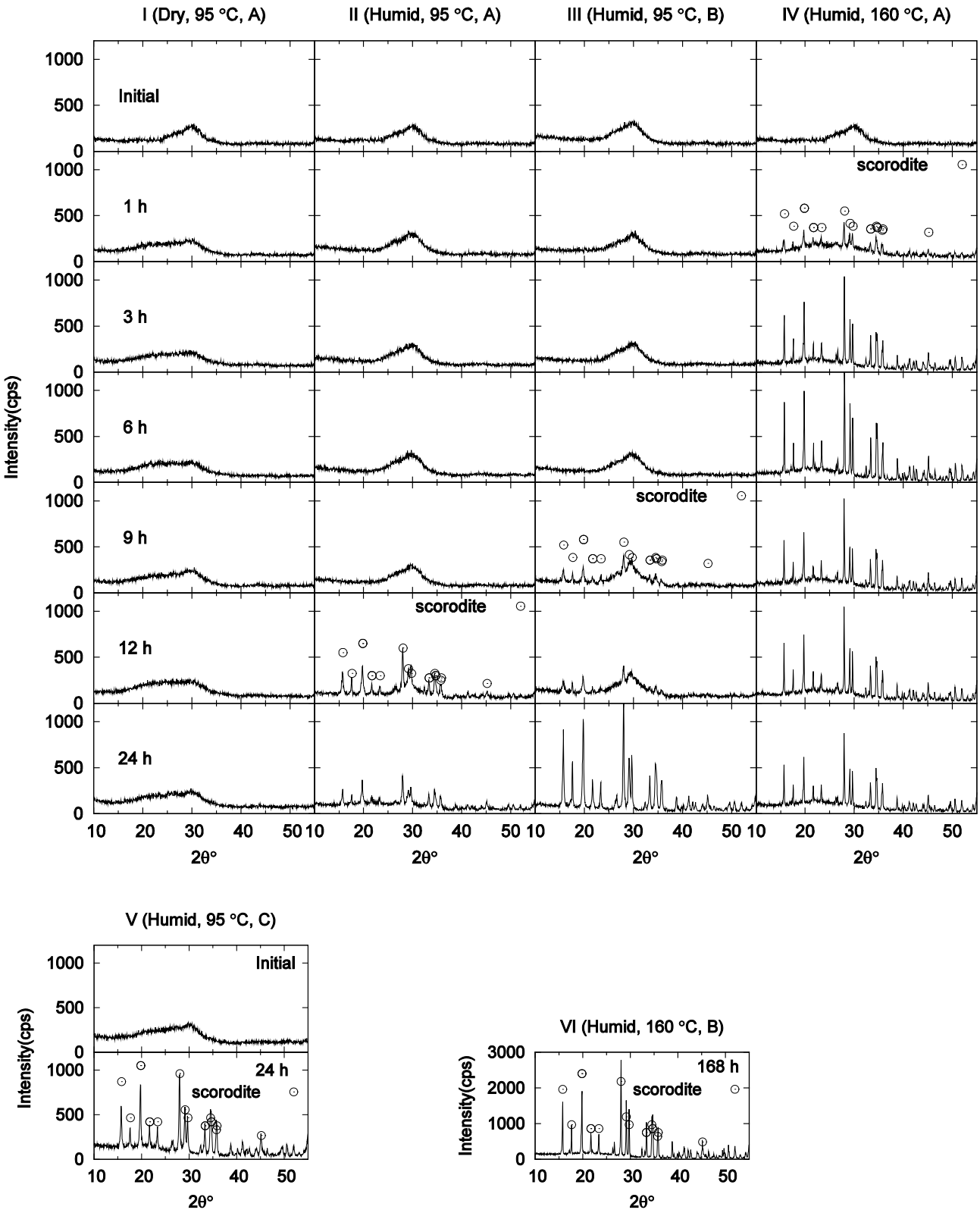

Figure 2. The XRD patterns of the samples obtained in all the experimental conditions and the retention times.

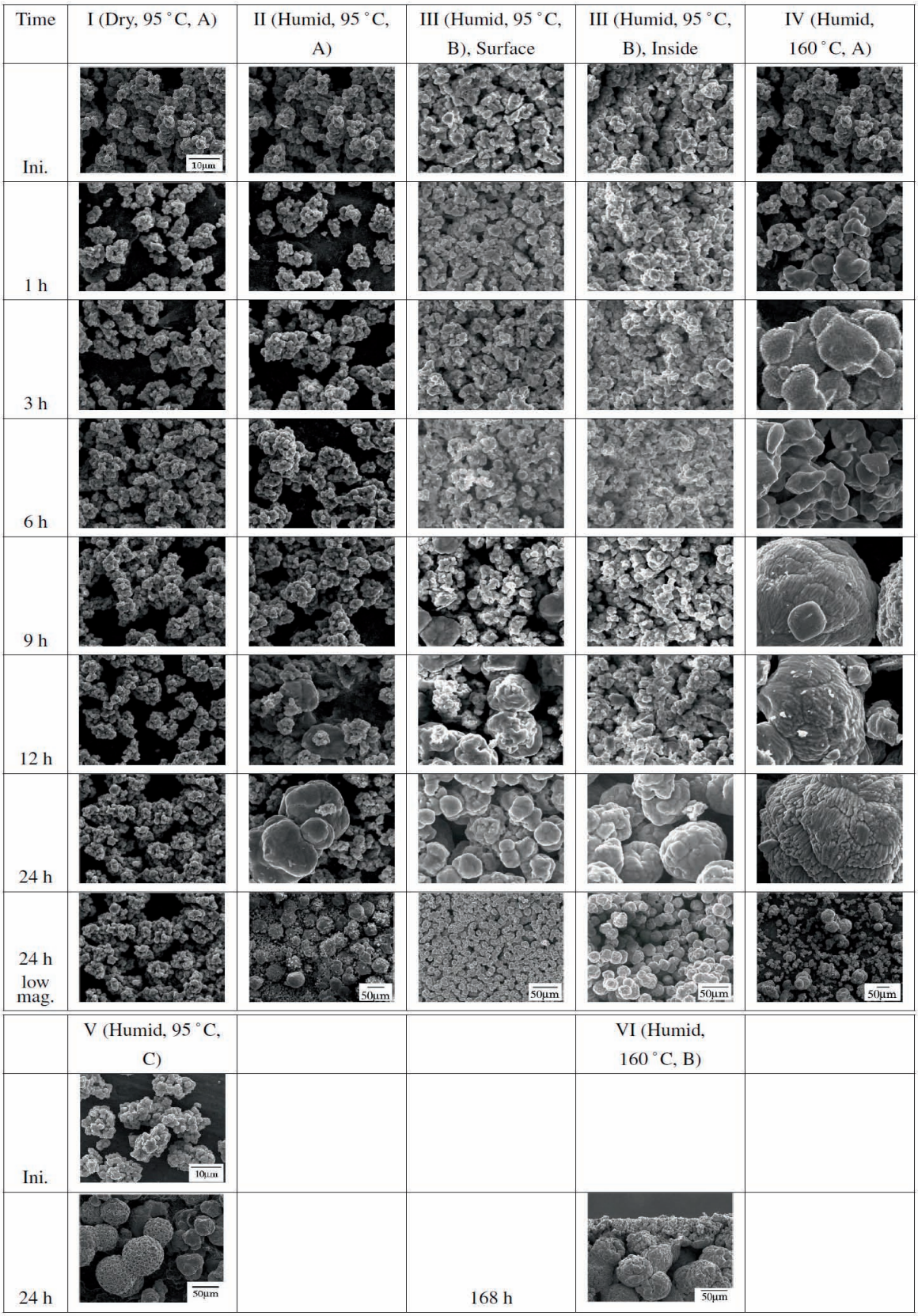

Figure 3. The SEM images of the samples obtained in all the experimental conditions and the retention times.

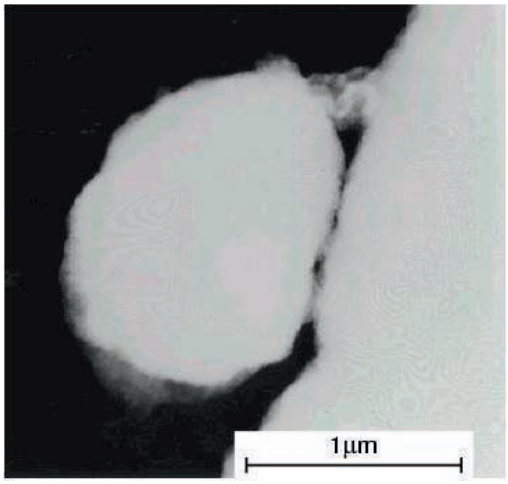

(a)

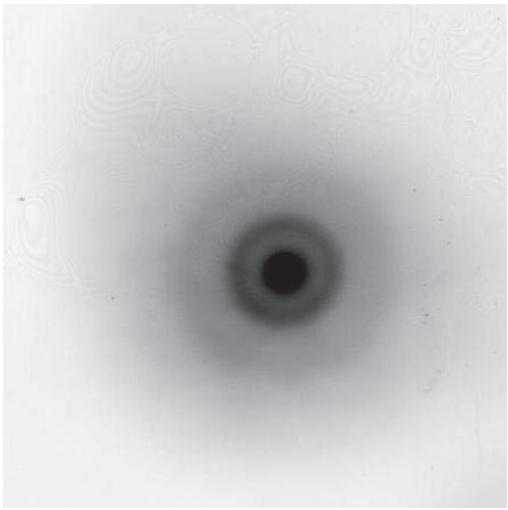

(b)

Figure 4. The TEM observation results for the initial sample A. (a) Bright field image, (b) electron beam diffraction pattern.

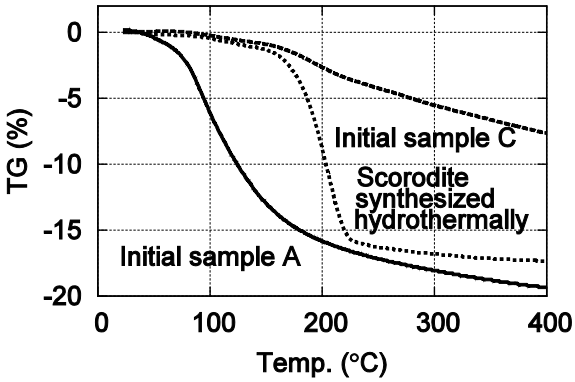

Figure 5. The results of thermo-gravimetry analysis for the initial samples A and C. The result of the hydrothermally synthesized scorodite at 160°C is shown as a reference.

3.2 Crystallization and Morphology of the Sample in Each Experimental Condition

3.2.1 Experiment I

The sample A was retained in the dry atmosphere at 95°C. XRD patterns of sample obtained in experiment I are shown in Figure 2. After 1 h, intensity from 20° to 30° rose, and it was obvious that the pattern was the same to the initial sample C. Since no remarkable change was observed until 24 h, it was found that crystallization did not occur in the dry atmosphere. SEM images in Figure 3 showed that there was not the remarkable change from the initial sample until 24 h.

TG results of the sample after the experiment are shown in Figure 6(a). It was observed that the mass reduction decreased with increase in the retention time. It was confirmed that the dehydration progressed at 95°C in the dry atmosphere.

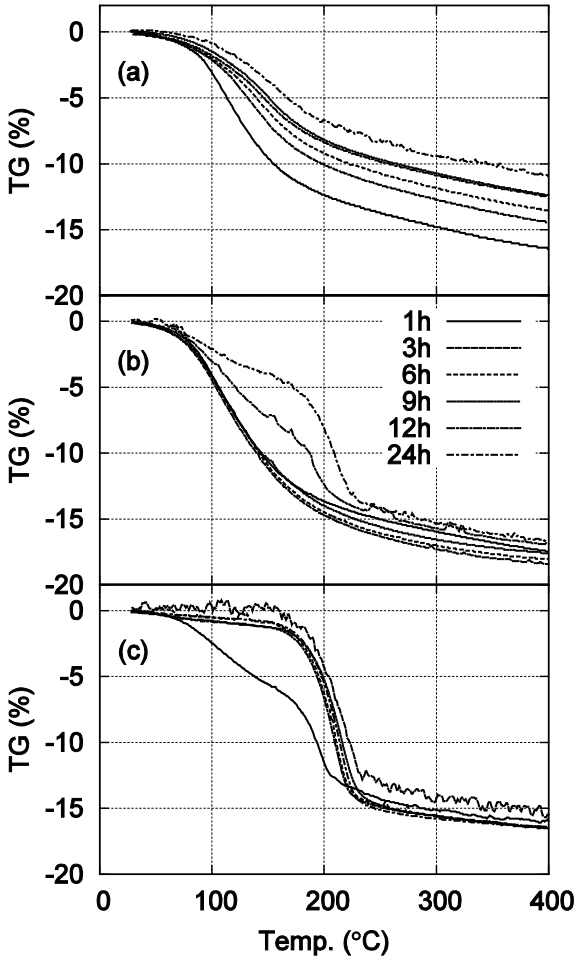

Figure 6. The results of thermo-gravimetry analysis for the samples after the experiments. (a) Experiment I (Dry, 95°C, A), (b) Experiment II (Humid, 95°C, A), (c) Experiment IV (Humid, 160°C, A).

3.2.2 Experiment II

The sample A was retained in the saturated steam atmosphere at 95°C. XRD patterns of samples obtained in experiment II are shown in Figure 2. Because any peaks were not seen until 9 h, it was understood that the sample remained as amorphous. At the retention times of 12 and 24 h, peaks were observed in corresponding to the scorodite. It was found that the crystallization of the amorphous to the scorodite occurred in 12 h.

From SEM images in Figure 3 at the retention time from 1 h to 9 h, agglomerates consisting of particles with diameter of 1 μm were observed, which were the same as the initial sample. Some particles of around 10 μm in diameter appeared at the retention time of 12 h. The retention time was the same to the time when the crystallization started to be detected in the XRD pattern. At the retention time of 24 h, the particles of 40 μm in diameter were observed. It was found the particle grew with retention time. However, many particles unchanged from the beginning were also observed.

A particle of 30 μm in diameter obtained at 24 h was cut by FIB (focused ion beam) and the cross section was observed. A SEM image is shown in Figure 7. Although small pores and striation-shaped cracks were observed, the particle was found to be dense as a whole. Forming a particle of 30 μm requires 27,000 ($= 30^3$) particles of 1 μm. It is surprised to know that such particles were formed at a low temperature as 95°C.

Figure 8 shows the TEM observation result of a part of cross section which was obtained by cutting a particle of 30 μm with FIB. The dark field image indicated that there were multiple regions in the size from 100 nm to 500 nm. The electron beam diffraction pattern revealed that each region was a crystallite and had a different orientation from other regions. Therefore, it may be said that the particle of 30 μm was not a single crystal but a polycrystal consisting of crystallites with the size of the 500 nm order.

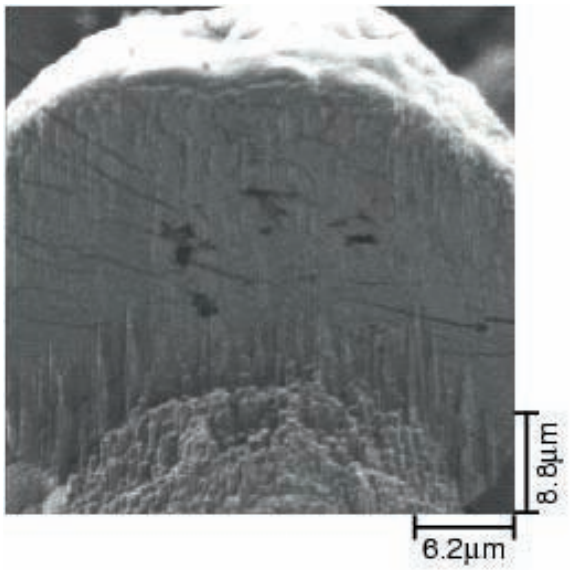

Figure 7. The cross sectional SEM image of a 30 μm particle obtained in the experiment II (Humid, 95°C, A) at 24 h. The cross section was obtained by cutting the particle with FIB.

The TEM observation results of a particle of around 1 μm are shown in Figure 9. It was found from the electron beam diffraction pattern that the particle was amorphous. This particle was the same to the particle of the initial sample in size and shape. Consequently, a possibility is suggested that crystallization is hard to progress if the particle size remains the same to the initial particle.

The TG result of the sample after the experiment is shown in Figure 6(b). The TG curves of the samples until 9 h were in the same to that of the initial sample. At the retention times of 12 and 24 h, mass reduction decreased below 160°C and increased from 160°C to 220°C. The reduction was due to the dehydration from the amorphous below 160°C and mainly from the crystal in the temperature range between 160°C and 220°C. From the mass reduction in the two temperature ranges, crystal fraction was roughly estimated as 56% at 12 h and 78% at 24 h.

3.2.3 Experiment III

The effect of the pressure forming was investigated in the experiment III. From the XRD result shown in Figure 2, scorodite was detected at 9 h and the peak intensities became higher at 24 h. In comparison with the case of experiment II, crystallization started in a shorter time and the intensities at 24 h were higher. Accordingly the pressure forming was found to accelerate the crystallization.

The SEM image is shown in Figure 3. Particles of around 10 μm were observed in the disc surface at 9 h. The retention time agreed with the time when the peaks of scorodite appeared in the XRD pattern. The particle size was about 5 μm at 24 h and the initial particles of 1 μm were not observed, showing high homogeneity. It can be said that the small particles of the initial size decreased with progress of the retention time and the fraction of the large particles increased. The reason the particle size did not increase monotonically with the retention time might be that the contact situation between the particles after the pressure forming differed in each sample.

Inside the disc, all particles were of 1um even at 12 h, but grew to 20 μm at 24 h with high homogeneity. At 24 h, the particles inside the disk were larger than those on the disk surface.

3.2.4 Experiment IV

The effect of temperature was investigated in the experiment IV. From the XRD result shown in Figure 2, scorodite

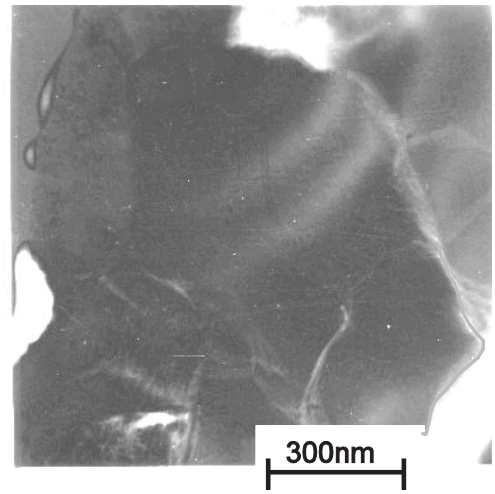

(a)

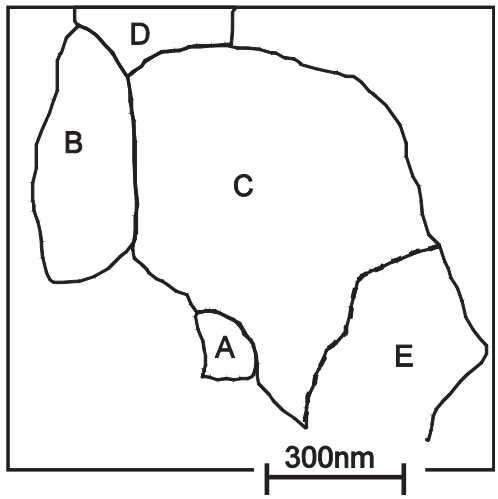

(b)

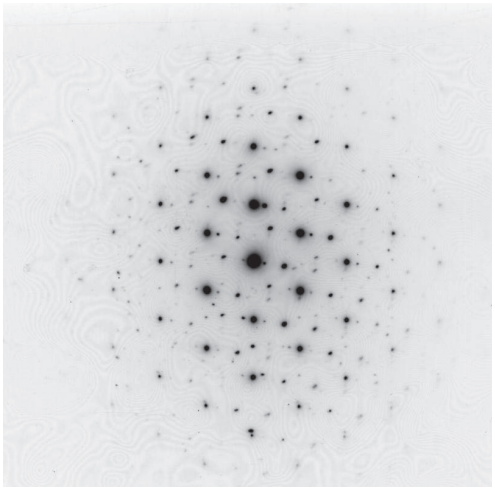

(c)

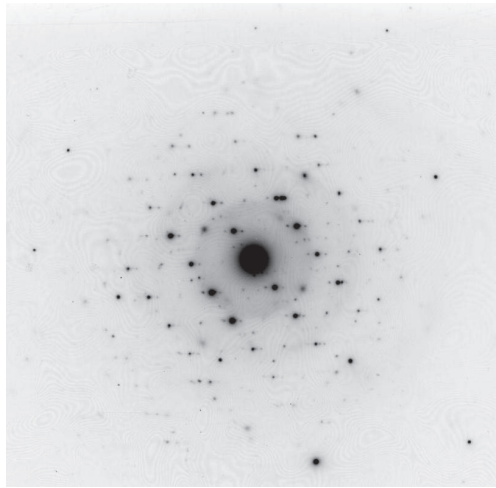

(d)

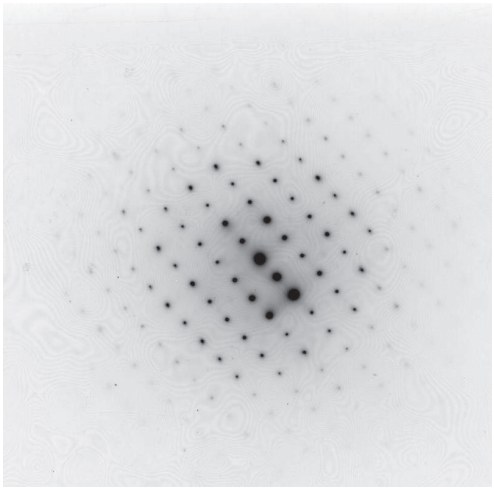

(e)

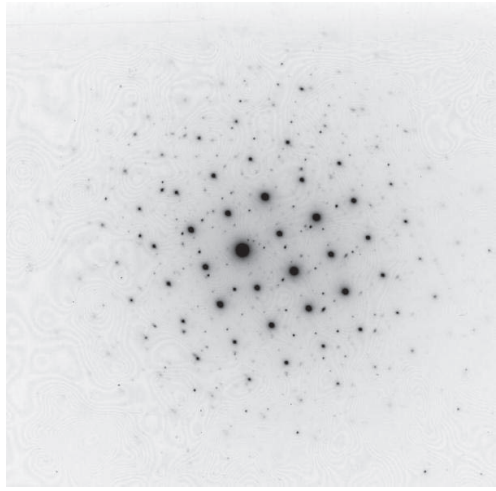

(f)

Figure 8. The TEM observation result of a 30 μm particle obtained in experiment II (Humid, 95°C, A) at 24 h. The cross section was obtained by cutting the particle with FIB. (a) Dark field image, (b) schematic view, Electron beam diffraction patterns (c) in region A, (d) in region B, (e) in region C, (f) in region D.

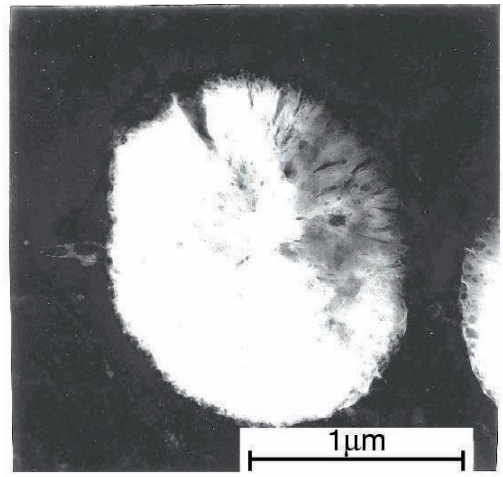

(a)

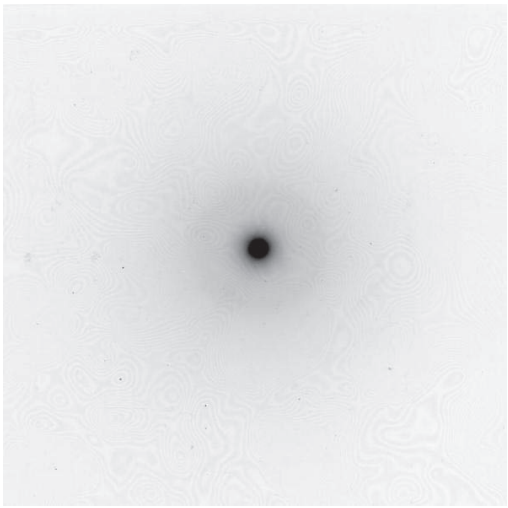

(b)

Figure 9. TEM observation results of a 1 μm particle obtained in experiment II (Humid, 95°C, A) at 24 h. (a) Bright field image, (b) electron beam diffraction pattern.

was detected at 1 h. The peak intensities increased until 6 h, followed by a slight decrease until 24 h. In comparison with the case of experiment II, crystallization started in a shorter time and the intensities at 24 h were higher. Consequently, it is clear that the higher retention temperature is effective in promoting crystallization.

From the SEM image in Figure 3, particles of 10 μm were partly formed already in 1h, which agreed with the time when the peaks of scorodite appeared in XRD. The particle size increased with time and the particles of 50 μm were seen at 24 h. However, as seen in the image in a low magnification, weak agglomerates consisting of the particles of 10 μm were also observed even at 24 h. It seems that the local difference in the contact situation may influence the particle size. In any cases of retention time, the particles were larger than that in the experiment II, showing that higher temperature is effective in obtaining larger particles.

The TG results of the samples after the experiments are shown in Figure 6(c). Even at the retention time of 1h, mass reduction decreased below 160°C and increased in the range between 160°C and 220°C. From the mass reduction, the crystal fraction was roughly estimated as 67% at 1 h, and as 100% at 3 h and longer.

3.2.5 Experiment V

The dehydrated initial sample C was used in the experiment V. From the XRD result shown in Figure 2, scorodite was detected at 24 h and the peak intensities were higher than that of experiment II at 24 h. The SEM image in Figure 3 shows that particles of 60 μm were formed. There were two types of particles; one with surface having intense irregularity and the other with the smooth surface.

The results of the experiment V clearly show that the amorphous dehydrated ferric arsenate can also be transformed to scorodite by taking water under saturated steam atmosphere at 95°C. It was also confirmed that even in this case the particles became larger than the initial sample.

3.2.6 Experiment VI

In the experiment VI, the initial sample B (powder compact) was retained at 160°C for 168 h. From the XRD result in Figure 2, scorodite was detected and the peak intensities were higher than those of other experiments.

The SEM image of the cross section is shown in Figure 3. The inside of the disk was composed of particles of 60 μm. There was a layer near the disk surface with the thickness of 50 μm, composed of particles of 5 μm. It was revealed that except the surface layer the particle size was large and uniform compared with other experiments.

3.3 Summary of the Variation with Time in Particle Size and the Crystallinity

As a summary of the experimental results described in Section 3.2, transitions of the particle size and the XRD peak intensity are shown in Figure 10. The average size of the larger particles observed with SEM is shown in Figure 10(a). Peak intensity at $2\theta = 19.8°$ corresponding to a scorodite peak is shown in Figure 10(b). In addition, half-band width (full width at half maximum) of the peak is shown in Figure 10(c). In comparison, those values of the hydrothermally synthesized scorodite were plotted.

In Figure 10(a), the time when the particle size began to increase was long in 95°C and short in 160°C. The particle size increased with time but showed saturated tendency.

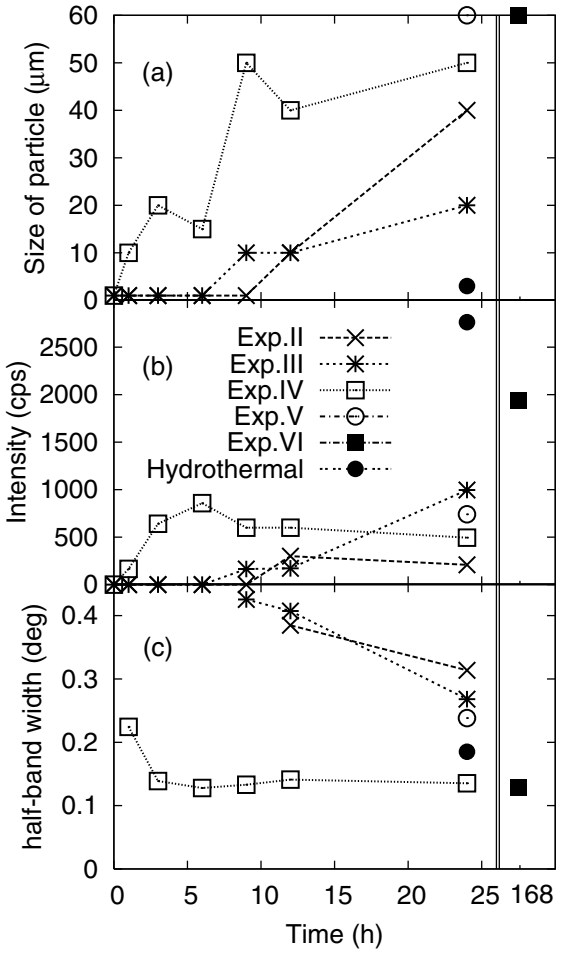

Figure 10. The transitions of (a) the particle size, (b) the XRD peak intensity, (c) the half-band width of the peak at $2\theta = 19.8°$.

The time when the peak began to be observed in Figure 10(b) was coincident with the time when the particle begins to grow big in Figure 10(a). Although the amorphous hydrated ferric arsenate is metastable with higher free energy than the scorodite, it is thought that the specific surface energy of the crystal is higher than that of amorphous. Therefore, when the amorphous becomes the crystal, the particle size may increase to decrease the specific surface area and hence the total surface energy. On the contrary, if the particle size unchanged, crystallization might be hard because the total surface energy increases with increase in the specific surface energy.

As shown in Figure 10(b), the diffraction intensity generally increased with time. In the experiments II and IV, it showed the maximum and decreased slightly afterwards. The increase in the intensity with time might be caused by the increase in the crystal fraction as showed in Figure 6 and by the improvement of the crystalline integrity. As shown in Figure 10(c), the half-band width decreased with time, confirming the improvement of the crystalline integrity. The half-band width in the experiment IV became constant after 3 h.

The intensity in the experiment II slightly decreased from 12 h to 24 h. In the period, it was expected that the intensity became higher because the crystal fraction increased as shown in Figure 6(b) and the half-band width decreased as shown in Figure 10(c). Therefore, it seems that intensity might decrease due to the growth of particles shown in Figure 10(a). The attenuation length [11] of the Cu Kα line for scorodite is 5 μm at $2\theta = 19.8°$. Because the length is smaller than the size of the generated scorodite, an absorption effect of X-ray might somehow decrease the intensity with increase in the particle size. Similarly, in the case of experiment IV, the intensity decreased after 6 h. In the period, the crystal fraction was constant at 100% as shown in Figure 6(c) and the half-band width was constant as shown in Figure 10(c). The decrease in the intensity seems to be caused by the increase in the particle size.

The diffraction intensity was high at 1940 in the experiment VI, and the diffraction intensity of the hydrothermally synthesized scorodite was higher at 2760. Since the particle size of the hydrothermally synthesized scorodite was 3 μm, it is thought that the effect of the absorption effect was small. In addition, the compact samples after the experiments III and VI were cracked with the pestle and mortar for the XRD analyses. It seems that the cracking made the particle size smaller and caused higher intensity. Based upon the foregoing, the crystallinity cannot be judged from the intensity data for the XRD samples in this study.

As shown in Figure 10(c), the half-band width of the experiment VI was as small as the experiment IV. In comparison with experiments II, III and V at 95°C, the half-band width in the experiments IV and VI at 160°C was small, meaning high crystallinity. Since the half-band width of the sample obtained at 160°C was slightly smaller than that of the hydrothermally synthesized scorodite, the crystallinity of the scorodite obtained in the saturated steam atmosphere was found to be high.

4 Conclusions

As a part of the mechanism elucidation of scorodite formation, the amorphous ferric arsenate was retained in the gas atmospheres. The influences of the atmosphere and temperature were investigated on the transition in the crystallinity and particle size. The following results were obtained:

(1) In the dry atmosphere, the crystallization did not occur. The particle size did not change.

(2) In the saturated steam atmosphere, the crystallization occurred at both 95°C and 160°C.

(3) The pressure forming of the sample shortened the incubation period for the crystallization.

(4) The higher temperature accelerated the crystallization in terms of the incubation period and crystallinity.

(5) The dehydrated amorphous ferric arsenate was transformed to scorodite under steam saturation at 95°C.

(6) The crystallinity of the sample formed at 160°C for 3 h was the same as that of the hydrothermally synthesized scorodite.

(7) The start of the crystallization was coincident with the start of the increase in particle size. It suggested that the increase in particle size contributed to the crystallization.

References

[1] J. E. Dutrizac and J. L. Jambor, The synthesis of crystalline scorodite, $FeAsO_4{\cdot}2H_2O$, *Hydrometallurgy*, **19** (1988), 377–384.

[2] G. P. Demopoulos, F. Lagno, Q. Wang and S. Singhania, The atmospheric scorodite process, *COPPER 2003 – COBRE 2003, Vol. VI – Hydrometallurgy of Copper (BOOK 2)*, METSOC, (2003), pp. 597–616.

[3] T. Fujita, R. Taguchi, M. Abumiya, M. Matsumoto, E. Shibata and T. Nakamura, Novel atmospheric scorodite synthesis by oxidation of ferrous sulfate solution. Part II. Effect of temperature and air, *Hydrometallurgy*, **90** (2008), 85–91.

[4] T. Fujita, R. Taguchi, M. Abumiya, M. Matsumoto, E. Shibata and T. Nakamura, Novel atmospheric scorodite synthesis by oxidation of ferrous sulfate solution. Part I, *Hydrometallurgy*, **90** (2008), 92–102.

[5] T. Fujita, R. Taguchi, M. Abumiya, M. Matsumoto, E. Shibata and T. Nakamura, Effects of zinc, copper and sodium ions on ferric arsenate precipitation in a novel atmospheric scorodite process, *Hydrometallurgy*, **93** (2008), 30–38.

[6] T. Fujita, R. Taguchi, M. Abumiya, M. Matsumoto, E. Shibata and T. Nakamura, Effect of pH on atmospheric scorodite synthesis by oxidation of ferrous ions: Physical properties and stability of the scorodite, *Hydrometallurgy*, **96** (2009), 189–198.

[7] T. Fujita, R. Taguchi, E. Shibata and T. Nakamura, Preparation of an As(V) solution for scorodite synthesis and a proposal for an integrated As fixation process in a Zn refinery, *Hydrometallurgy*, **96** (2009), 300–312.

[8] K. Shinoda, T. Tanno, T. Fujita and S. Suzuki, Coprecipitation of large scorodite particles from aqueous Fe(II) and As(V) solution by oxygen injection, *Materials Transactions*, **50** (2009), 1196–1201.

[9] H. Itou, T. Takasu, T. Nakamura, E. Shibata and H. Tateiwa, Mechanism of scorodite formation at ambient temperature as determined by TEM analysis, *Proceedings of the third International Symposium on Iron Control in Hydrometallurgy*, METSOC, (2006), pp. 897–909.

[10] E. Krause and V. A. Ettel, Solubility and stability of scorodite, $FeAsO_4{\cdot}2H_2O$: New data and further discussion, *American Mineralogist*, **73** (1988), 850–854.

[11] B. L. Henke, E. M. Gullikson and J. C. Davis, X-ray interactions: photoabsorption, scattering, transmission, and reflection at $E = 50$–30000 eV, $Z = 1$–92, *Atomic Data and Nuclear Data Tables*, **54** (1993), 181–342.